PHYSICAL REVIEW B **85**, 220504(R) (2012)

Evidence for an *s*-wave superconducting gap in $K_xFe_{2-y}Se_2$ from angle-resolved photoemission

M. Xu,[1] Q. Q. Ge,[1] R. Peng,[1] Z. R. Ye,[1] Juan Jiang,[1] F. Chen,[1] X. P. Shen,[1] B. P. Xie,[1] Y. Zhang,[1,*] A. F. Wang,[2] X. F. Wang,[2] X. H. Chen,[2] and D. L. Feng[1,†]

[1]*State Key Laboratory of Surface Physics, Department of Physics, and Advanced Materials Laboratory, Fudan University, Shanghai 200433, People's Republic of China*

[2]*Hefei National Laboratory for Physical Sciences at Microscale and Department of Physics, University of Science and Technology of China, Hefei, Anhui 230026, China*

(Received 15 May 2012; revised manuscript received 11 June 2012; published 20 June 2012)

Although a nodeless superconducting gap has been observed on the large Fermi pockets around the zone corner in $K_xFe_{2-y}Se_2$, whether its pairing symmetry is *s* wave or nodeless *d* wave is still under intense debate. Here we report an isotropic superconducting gap distribution on the small electron Fermi pocket around the *Z* point in $K_xFe_{2-y}Se_2$, which favors the *s*-wave pairing symmetry.

DOI: 10.1103/PhysRevB.85.220504 PACS number(s): 74.70.Xa, 74.25.Jb, 79.60.−i, 71.20.−b

Compared with the cuprate superconductors, the iron-based high-temperature superconductors (Fe-HTS's) exhibit much more diversified structures and electronic structures, which provide a rich playground for various competing instabilities. As a result, the pairing symmetry of the Cooper pair, one of the most fundamental characters of a superconductor, is still far from well understood for Fe-HTS's. For the Fe-HTS's whose Fermi surface is composed of hole pockets in the Brillouin zone center and electron pockets at the zone corner, *s*-wave pairing has been generally established not only in systems with nodeless superconducting gaps, such as $Ba_{1-x}K_xFe_2As_2$, $BaFe_{2-x}Co_xAs_2$, and $FeTe_{1-x}Se_x$,[1–5] but also even in ones with nodal superconducting gap, such as $BaFe_2(As_{1-x}P_x)_2$[6] and heavily overdoped $Ba_{1-x}K_xFe_2As_2$.[7] However, theoretically, whether there is a sign change or not for the order parameter in different Fermi sheets is still unsettled. For example, it could depend on whether spin fluctuations[8,9] or orbital fluctuations[10] are taken as the dominating pairing force. Moreover, for the recently discovered $A_xFe_{2-y}Se_2$ (A = K, Cs, Rb, ...) superconductor,[11–13] its parent compound[14,15] and electronic structure are both rather different from those of other Fe-HTS's,[16–18] and whether its pairing symmetry is *s* wave or nodeless *d* wave is currently under intense debate.[19–31] Therefore, a unified theme for the pairing symmetry in the Fe-HTS's has not been reached.

Let us take $K_xFe_{2-y}Se_2$ as an example. Its Fermi surface is made of a small electron pocket (κ) around *Z* and large electron cylinders (δ and δ') at the zone corners, as reported earlier and shown in Fig. 1(a).[15] A large and isotropic superconducting gap of ∼10 meV has been observed for the δ/δ' electron pockets, while a gap of ∼7 meV has been observed on the κ pocket due to the screening effect.[16] The lack of hole pockets near the zone center rules out the common $s^{\pm}$ pairing symmetry proposal based on scattering between the hole and electron Fermi surface sheets in the iron pnictides. Theories based on local antiferromagnetic exchange interactions have predicted *s*-wave pairing symmetry in this system that can account for the experimental results.[19–24] However, calculations based on the scattering among the δ/δ' electron pockets have indicated that the *d*-wave pairing channel would win over the *s*-wave pairing channel,[26–30] which makes the superconducting order parameters change sign between the neighboring δ/δ' Fermi pockets as illustrated in Fig. 1(b). Because the nodes would appear along the four $(0,0)-(\pm\pi,\pm\pi)$ directions (dashed lines) that do not cross any of the δ/δ' Fermi cylinders, it can explain the observed nodeless gap structure on the δ/δ' electron pockets. So far, these two pairing scenarios have not been distinguished experimentally.

Note that in Fig. 1(b) the nodal lines in the *d*-wave pairing scenario actually cross the κ pocket. One would expect nodes in the superconducting gap at such crossings but the gap to be nodeless in the *s*-wave pairing scenario. Therefore, the superconducting gap distribution of the κ pocket could serve as a benchmark to determine the pairing symmetry of $K_xFe_{2-y}Se_2$. Previously, because of the small size of the κ Fermi pocket, the detailed distribution of its gap was not reported. We here report the angle-resolved photoemission spectroscopy (ARPES) measurements on the detailed superconducting gap on the κ Fermi pocket in a $K_xFe_{2-y}Se_2$ superconductor. We found an isotropic superconducting gap of ∼8 meV, which favors the *s*-wave pairing symmetry. This work, together with previous studies,[16] suggests that the pairing symmetry of all the Fe-HTS's discovered so far is ubiquitously *s* wave.

$K_xFe_{2-y}Se_2$ single crystals were synthesized by the self-flux method as described elsewhere in detail,[12] which show flat shiny surfaces with dark black color. The superconducting sample shows the superconducting transition temperature (T_c) of ∼31 K. The chemical compositions of the samples were determined by energy-dispersive x-ray (EDX) spectroscopy to be $K_{0.77}Fe_{1.65}Se_2$. As shown earlier,[15,32] although there is a microscopic phase separation between the superconducting phase and the vacancy-ordered insulating phase in superconducting $K_xFe_{2-y}Se_2$ compounds, it does not affect the photoemission signal near the Fermi energy (E_F) from the superconducting phase due to screening. The synchrotron ARPES experiments were performed at Beamline 5-4 of the Stanford Synchrotron Radiation Lightsource (SSRL) facility and Beamline 21B1 of the National Synchrotron Radiation Research Center (NSRRC) facility, with Scienta R4000 electron analyzers. The overall energy resolution in the gap measurement is ∼10 meV at NSRRC, and angular resolution is ∼0.3 deg. The polarization dependence of the Fermi surface was measured at the Ultraviolet Synchrotron Orbital Radiation (UVSOR) facility with an MBS A-1 electron analyzer. The samples

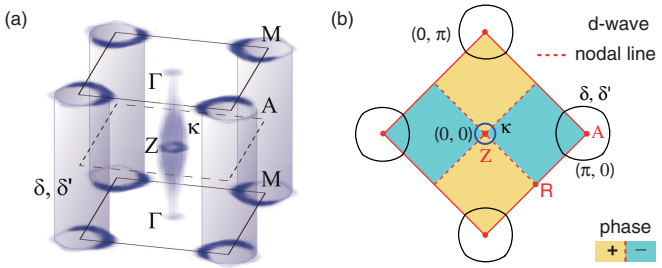

FIG. 1. (Color online) (a) The Fermi surface topology of $K_xFe_{2-y}Se_2$ superconductor in the three-dimensional (3D) Brillouin zone corresponding to two iron ions per unit cell. (b) Schematic diagram of the d-wave theoretical gap symmetry with the nodal lines along the $(0,0)-(\pm\pi,\pm\pi)$ directions. Positive and negative phases of the superconducting order parameter are denoted by different colors. The Fermi surface is based on the data in Fig. 2(b).

were cleaved *in situ* and measured under ultra-high-vacuum of 5×10^{-11} torr.

For a close examination of the κ electron pocket, Figs. 2(a) and 2(b) show the photoemission intensity maps for the Fermi surface at two different k_z values. Although the electron pockets around the zone corner show little k_z dependence, the small κ pocket could be only observed near the Z point for $k_z=\pi$, indicating its strong three-dimensional (3D) character. The spot at Γ is the residual weight of the κ band above E_F. The k_z dependence of κ is further illustrated by the photoemission intensity map along the k_y-k_z cross section of the Brillouin zone [Fig. 2(c)]. We determined the Fermi crossings of κ according to the momentum distribution curves (MDCs) near E_F taken with different photon energies [Fig. 2(d)]. The diameter of the κ pocket in the $k_z=\pi$ plane is about 0.22 $Å^{-1}$. Such a small enclosed κ electron pocket around Z is generally overlooked by theories in studying the pairing symmetry of $K_xFe_{2-y}Se_2$, even it was found to exhibit a superconducting gap with comparable amplitude as that on the large δ/δ' electron cylinders at the zone corner.

Previous photoemission studies on $K_xFe_{2-y}Se_2$ only resolved one electron pocket around the zone corner. In the folded Brillouin zone with two iron ions per unit cell, there should be two electron cylinders around the zone corner due to folding. Band calculations show that these two electron cylinders in $K_xFe_{2-y}Se_2$ have opposite symmetries with respect to the Z-Γ-M plane,[33] as found in other Fe-HTS's. To resolve this discrepancy, we show the polarization-dependent ARPES data in Figs. 2(e) and 2(f).[34] Due to the multiorbital nature of the Fermi surface in iron-based superconductors, a certain Fermi surface sheet might exhibit either even or odd spatial symmetry and thus could be observed in the p or s polarization geometry.[35] In the polarization-dependent ARPES studies of $BaFe_{2-x}Co_xAs_2$ and NaFeAs, one squarelike electron pocket and one elliptical electron pocket could be separately probed around the zone corner in the p and s polarization geometries, respectively.[35,36] Here in Figs. 2(e) and 2(f), there is an electron pocket around A in both p and s polarization geometries, indicating the existence of two electron pockets with opposite symmetries. Moreover, unlike the electron pockets observed in other Fe-HTS's, the two electron pockets could not be resolved in momentum, which indicates a low ellipticity and high

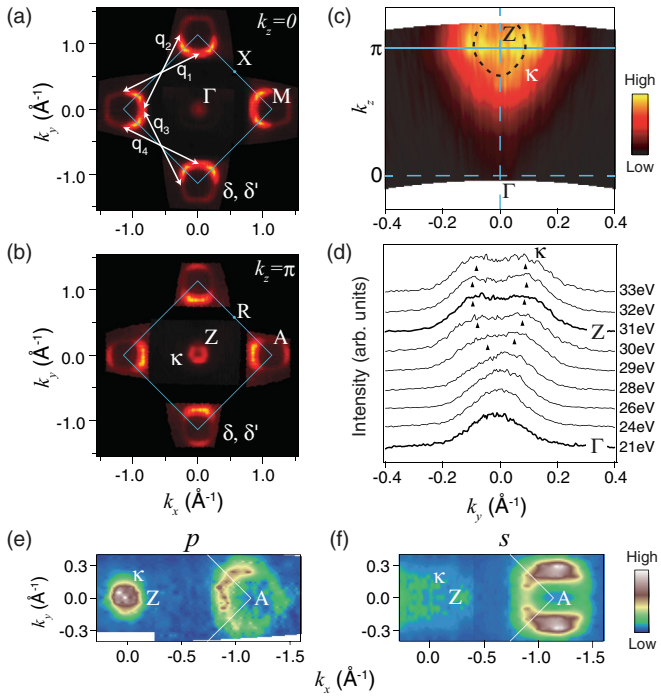

FIG. 2. (Color online) Fermi surface of $K_xFe_{2-y}Se_2$ superconductor. (a) The photoemission intensity map for the Fermi surface at $k_z=0$ taken with 21-eV photons at 35 K. The k_x and k_y are defined along Fe-Fe directions. (b) The photoemission intensity map for the Fermi surface at $k_z=\pi$ taken with 31-eV photons at 35 K. (c) The photoemission intensity map taken along k_y-k_z cross section of the 3D Brillouin zone. (d) The momentum distribution curves (MDCs) at Fermi energy (E_F) taken at different photon energies. (e), (f) The polarization dependence of the photoemission intensity maps taken in the Z-A plane at 35 K with the p and s polarization geometries, respectively. The arrows in panel (a) represent the nesting wave vectors $q_1=(\pi, 0.52\pi)$, $q_2=(0.52\pi, \pi)$, $q_3=(0.52\pi, -\pi)$, and $q_4=(-\pi, 0.52\pi)$ between the relatively straight sections of neighboring electron pockets. Data were taken at SSRL for panels (a)–(d) and UVSOR for panels (e) and (f).

degeneracy of these two electron pockets in $K_xFe_{2-y}Se_2$. This explains why only one electron pocket could be observed with the mixed polarization geometry in previous photoemission studies. Having obtained the 3D Fermi surface of $K_xFe_{2-y}Se_2$, one can estimate the carriers contributed by κ are about 0.002 electrons per Fe, and those by both δ and δ' are 0.202 electrons per Fe, assuming there is no iron vacancy in the superconducting phase.[37]

In the d-wave pairing scenario, the superconducting order parameter in the neighboring quarters has opposite signs in the unfolded Brillouin zone. It has been argued that in the folded Brillouin zone, where there are two iron ions in one unit cell, the folding of electron cylinders from one quarter to its neighboring quarter could induce hybridization and thus extra nodes.[38] However, this might not be the case here, due to the low ellipticity, little k_z dispersion, and weak interactions between the δ/δ' electron pockets. Therefore, the isotropic and nodeless superconducting gap distributions on the δ/δ' pockets might not be viewed as a conclusive evidence against the d-wave pairing symmetry in $K_xFe_{2-y}Se_2$.

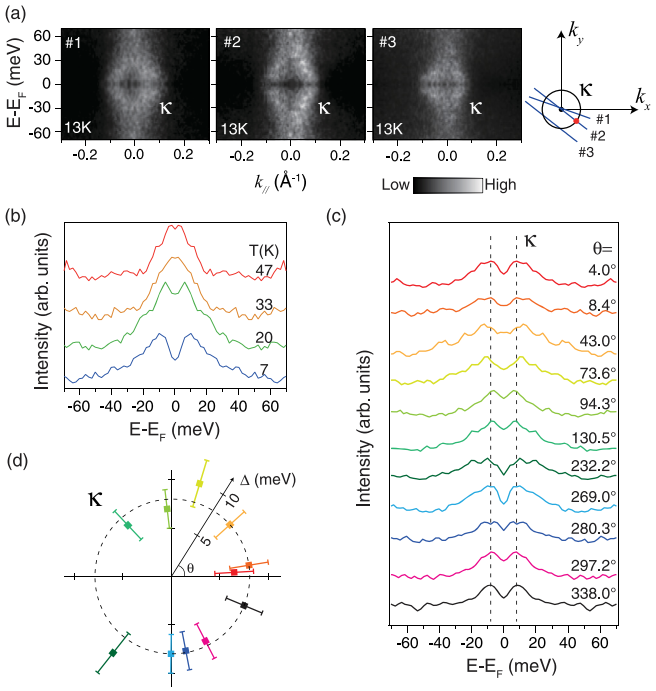

FIG. 3. (Color online) The superconducting gap at the κ pocket of $K_xFe_{2-y}Se_2$. (a) Symmetrized photoemission intensities for three-momentum cuts across the κ pocket near Z, as shown by the blue lines labeled 1–3 in the inset. (b) Temperature dependence of symmetrized energy distribution curves (EDCs) at the Fermi crossing marked by the red dot in panel (a). (c) Symmetrized EDCs at the Fermi crossings of the κ band with momenta counterclockwise along the κ pocket as shown by the labeled polar angles. (d) Gap distribution of the κ pocket around Z in polar coordinates, where the radius represents the gap size, and the polar angle θ represents the position on the κ pocket with respect to the Z point, $\theta = 0$ being the Z–A direction. The gap is estimated through an empirical fit as described in detail in Ref. 6, and the error bars come from the standard deviation of the fitting process. The data were taken at NSRRC with 31-eV photons at 13 K for panels (a), (c), and (d) and at SSRL with 31-eV photons for panel (b).

We now turn to the detailed distribution of the superconducting gap around the κ pocket. Figure 3(a) shows the symmetrized photoemission intensities along several cuts across the κ pocket near Z. The electronlike band dispersion is clearly visible, and the suppression of intensity at E_F illustrates the opening of a gap. The temperature dependence of the symmetrized energy distribution curves (EDCs) in Fig. 3(b) further indicates that this gap is the superconducting gap that opens only below T_c. Figure 3(c) plots the EDCs in the superconducting state at various Fermi crossings of κ pocket around the Z point. Clear superconducting coherence peaks were observed at different momenta and they roughly share the same peak position of about ~8 meV as marked by the vertical dashed line in Fig. 3(c). The momentum distribution of the superconducting gap on κ is shown in Fig. 3(d), which clearly shows a nodeless isotropic superconducting gap distribution. Note that the momenta we chose here almost cover the entire κ pocket, so the gap nodes should not be missed if they had existed. Moreover, even though the

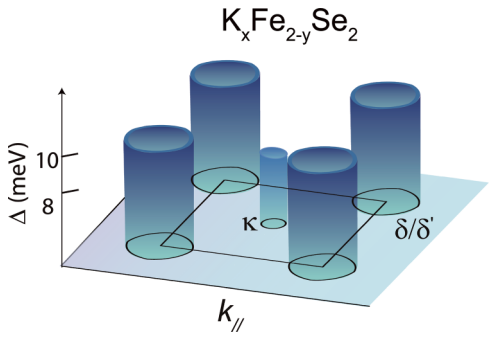

FIG. 4. (Color online) Summary of the superconducting gap distribution at κ, δ, and δ' pockets in $K_xFe_{2-y}Se_2$.

superconducting gap of iron pnictides often shows sizable k_z dependence[4,39] and even nodes on a hole Fermi surface,[6,7,40] our previous studies on $K_xFe_{2-y}Se_2$ have shown that the superconducting gap of κ is independent of k_z in the k_x-k_z plane.[16] Therefore, one would exclude the existence of any horizontal nodal line here. Together with the nodeless superconducting gap on δ/δ' electron pockets determined previously,[16] we conclude a nodeless superconducting gap structure in all Fermi surface sheets of $K_xFe_{2-y}Se_2$ as summarized in Fig. 4.

The observed nodeless isotropic superconducting gap on the κ Fermi pocket is consistent with the s-wave pairing symmetry, while it poses serious challenges to the d-wave pairing scenario in $K_xFe_{2-y}Se_2$. Although the existing theories that predict d-wave have neglected the contribution of the κ pocket, the interactions between δ/δ' and κ would most likely induce a phase change and thus nodes on κ. Considering the small density of states of κ, its large gap size is likely caused by the interaction with the δ/δ'. It is also possible that there is a d-wave pairing component in addition to the s-wave one, for example, in the $s + id$ pairing form.[31] However, the isotropic superconducting gaps on all the Fermi surface sheets indicate that the d component should be very weak.

Recently, a resonance mode has been observed in the inelastic neutron scattering studies of $Rb_xFe_{2-y}Se_2$,[41,42] which has been taken as a support for the d-wave pairing symmetry, where the order parameter of the large electron cylinders alternates its sign from one zone corner to the next as illustrated in Fig. 1(b).[28,29] Indeed, the resonance mode is located at the wave vectors of $(\pi,\pi/2)$ and $(\pi/2,\pi)$ that can match the q_1 and q_2 nesting wave vectors between the relatively straight Fermi surface sections in Fig. 2(a).[42] However, noting that there are two degenerate Fermi surface sheets at each zone corner, δ and δ', the resonance mode could be understood in the s-wave symmetry as well. Because although the sign of the superconducting order parameter of δ or δ' is fixed, they could be opposite as demonstrated in a recent theory,[31] and the interpocket scattering between the δ pocket at one zone corner and the δ' pocket at the neighboring corner will result in a resonance mode. In other words, the resonance mode can be taken as evidence for the sign change between the δ and δ' Fermi surfaces. Nevertheless, we also note that the very sharp momentum distribution of the resonance is rather different

from the usual behavior of resonance modes observed in other iron-based superconductors. It is not unlikely that the sharp resonance could be caused by some unknown dynamics in this rather complicated material, which demands further theoretical and experimental work.

To summarize, we have identified isotropic nodeless superconducting gap distribution on the κ Fermi pocket in $K_xFe_{2-y}Se_2$, which provides a strong experimental support to the *s*-wave pairing symmetry in this compound and agrees with theories based on local antiferromagnetic exchange interactions.[21] Our results indicate *s*-wave is likely a ubiquitous pairing symmetry of iron-based high-temperature superconductors in general.

We are grateful to Dr. D. H. Lu at SSRL, Dr. C. M. Cheng and Prof. K. D. Tsuei at NSRRC, Dr. M. Matsunami and Dr. S. Kimura at UVSOR for experimental assistance, and Prof. J. P. Hu, Prof. Z. D. Wang, Prof. J. X. Li, and Prof. Q. H. Wang for helpful discussions. This work is supported in part by the National Science Foundation of China and the National Basic Research Program of China (973 Program) under Grants No. 2012CB921400, No. 2011CB921802, and No. 2011CBA00112. SSRL is operated by the US DOE, Office of Basic Energy Science, Divisions of Chemical Sciences and Material Sciences. Part of this work was supported by the Use-of-UVSOR Facility Program of the Institute for Molecular Science.

*yanzhangfd@fudan.edu.cn

†dlfeng@fudan.edu.cn

[1] H. Ding, P. Richard, K. Nakayma, K. Sugawara, T. Arakane, Y. Sekiba, A. Takayma, S. Souma, T. Sato, T. Takahashi, Z. Wang, X. Dai, Z. Fang, G. F. Chen, J. L. Luo, and N. L. Wang, Europhys. Lett. **83**, 47001 (2008).

[2] H. Miao *et al.*, Phys. Rev. B **85**, 094506 (2012).

[3] T. Hanaguri, S. Niitaka, K. Kuroki, and H. Takagi, Science **328**, 474 (2010).

[4] Y. Zhang, L. X. Yang, F. Chen, B. Zhou, X. F. Wang, X. H. Chen, M. Arita, K. Shimada, H. Namatame, M. Taniguchi, J. P. Hu, B. P. Xie, and D. L. Feng, Phys. Rev. Lett. **105**, 117003 (2010).

[5] K. Terashima, Y. Sekiba, J. H. Bowen, K. Nakayama, T. Kawahara, T. Sato, P. Richard, Y. M. Xu, L. J. Li, G. H. Cao, Z. A. Xu, H. Ding, and T. Takahashi, Proc. Natl. Acad. Sci. USA **106**, 7330 (2009).

[6] Y. Zhang, Z. R. Ye, Q. Q. Ge, F. Chen, J. Jiang, M. Xu, B. P. Xie, and D. L. Feng, Nat. Phys. **8**, 371 (2012).

[7] W. Malaeb *et al.*, arXiv:1204.0326 (unpublished).

[8] I. I. Mazin, D. J. Singh, M. D. Johannes, and M. H. Du, Phys. Rev. Lett. **101**, 057003 (2008).

[9] K. Kuroki, S. Onari, R. Arita, H. Usui, Y. Tanaka, H. Kontani, and H. Aoki, Phys. Rev. Lett. **101**, 087004 (2008).

[10] H. Kontani and S. Onari, Phys. Rev. Lett. **104**, 157001 (2010).

[11] J. G. Guo, S. F. Jin, G. Wang, S. C. Wang, K. X. Zhu, T. T. Zhou, M. He, and X. L. Chen, Phys. Rev. B **82**, 180520 (2010).

[12] J. J. Ying, X. F. Wang, X. G. Luo, A. F. Wang, M. Zhang, Y. J. Yan, Z. J. Xiang, R. H. Liu, P. Cheng, G. J. Ye, and X. H. Chen, Phys. Rev. B **83**, 212502 (2011).

[13] M. H. Fang, H. D. Wang, C. H. Dong, Z. J. Li, C. M. Feng, J. Chen, and H. Q. Yuan, Europhys. Lett. **94**, 27009 (2011).

[14] W. Bao, Q. Z. Huang, G. F. Chen, M. A. Green, D. M. Wang, J. B. He, and Y. M. Qiu, Chin. Phys. Lett. **28**, 086104 (2011).

[15] F. Chen, M. Xu, Q. Q. Ge, Y. Zhang, Z. R. Ye, L. X. Yang, J. Jiang, B. P. Xie, R. C. Che, M. Zhang, A. F. Wang, X. H. Chen, D. W. Shen, J. P. Hu, and D. L. Feng, Phys. Rev. X **1**, 021020 (2011).

[16] Y. Zhang, L. X. Yang, M. Xu, Z. R. Ye, F. Chen, C. He, H. C. Xu, J. Jiang, B. P. Xie, J. J. Ying, X. F. Wang, X. H. Chen, J. P. Hu, M. Matsunami, S. Kimura, and D. L. Feng, Nat. Mater. **10**, 273 (2011).

[17] D. Mou *et al.*, Phys. Rev. Lett. **106**, 107001 (2011).

[18] X. P. Wang, T. Qian, P. Richard, P. Zhang, J. Dong, H. D. Wang, C. H. Dong, M. H. Fang, and H. Ding, Europhys. Lett. **93**, 57001 (2011).

[19] C. Fang, Y. L. Wu, R. Thomale, B. A. Bernevig, and J. P. Hu, Phys. Rev. X **1**, 011009 (2011).

[20] K. Seo, B. A. Bernevig, and J. P. Hu, Phys. Rev. Lett. **101**, 206404 (2008).

[21] J. P. Hu and H. Ding, Sci. Rep. **2**, 381 (2012).

[22] J. P. Hu and N. N. Hao, Phys. Rev. X **2**, 021009 (2012).

[23] X. Lu, C. Fang, W. F. Tsai, Y. Jiang, and J. P. Hu, Phys. Rev. B **85**, 054505 (2012).

[24] R. Yu, P. Goswami, Q. M. Si, P. Nikolic, and J. X. Zhu, arXiv:1103.3259 (unpublished).

[25] Y. Z. You, F. Yang, S. P. Kou, and Z. Y. Weng, Phys. Rev. Lett. **107**, 167001 (2011).

[26] F. Wang, F. Yang, M. Gao, Z. Y. Lu, T. Xiang, and D. H. Lee, Europhys. Lett. **93**, 57003 (2011).

[27] Y. Zhou, D. H. Xu, F. C. Zhang, and W. Q. Chen, Europhys. Lett. **95**, 17003 (2011).

[28] T. Das and A. V. Balatsky, Phys. Rev. B **84**, 014521 (2011).

[29] T. A. Maier, S. Graser, P. J. Hirschfeld, and D. J. Scalapino, Phys. Rev. B **83**, 100515 (2011).

[30] T. Zhou and Z. D. Wang, arXiv:1202.1607 (unpublished).

[31] M. Khodas and A. V. Chubukov, arXiv:1202.5563 (unpublished).

[32] A. Charnukha, A. Cvitkovic, T. Prokscha, D. Proepper, N. Ocelic, A. Suter, Z. Salman, E. Morenzoni, J. Deisenhofer, V. Tsurkan, A. Loidl, B. Keimer, and A. V. Boris, arXiv:1202.5446 (unpublished).

[33] X. W. Yan, M. Gao, Z. Y. Lu, and T. Xiang, Phys. Rev. B **84**, 054502 (2011).

[34] F. Chen, Q. Q. Ge, M. Xu, Y. Zhang, X. P. Shen, W. Li, M. Matsunami, S. Kimura, J. P. Hu, and D. L. Feng (unpublished).

[35] Y. Zhang, F. Chen, C. He, B. Zhou, B. P. Xie, C. Fang, W. F. Tsai, X. H. Chen, H. Hayashi, J. Jiang, H. Iwasawa, K. Shimada, H. Namatame, M. Taniguchi, J. P. Hu, and D. L. Feng, Phys. Rev. B **83**, 054510 (2011).

[36] Y. Zhang, C. He, Z. R. Ye, J. Jiang, F. Chen, M. Xu, Q. Q. Ge, B. P. Xie, J. Wei, M. Aeschlimann, X. Y. Cui, M. Shi, J. P. Hu, and D. L. Feng, Phys. Rev. B **85**, 085121 (2012).

[37] W. Li, H. Ding, Z. Li, P. Deng, K. Chang, K. He, S. H. Ji, L. L. Wang, X. C. Ma, J. P. Hu, X. Chen, and Q. K. Xue, arXiv:1204.1588 (unpublished).

[38]I. I. Mazin, Phys. Rev. B **84**, 024529 (2011).

[39]D. V. Evtushinsky, V. B. Zabolotnyy, T. K. Kim, A. A. Kordyuk, A. N. Yaresko, J. Maletz, S. Aswartham, S. Wurmehl, A. V. Boris, D. L. Sun, C. T. Lin, B. Shen, H. H. Wen, A. Varykhalov, R. Follath, B. Bchner, and S. V. Borisenko, arXiv:1204.2432 (unpublished).

[40]H. Kawano-Furukawa, C. J. Bowell, J. S. White, J. L. Gavilano, R. W. Heslop, A. S. Cameron, E. M. Forgan, K. Kihou, C. H. Lee, A. Iyo, H. Eisaki, T. Saito, H. Fukazawa, Y. Kohori, R. Cubitt, C. D. Dewhurst, and M. Zolliker, Phys. Rev. B **84**, 024507 (2011).

[41]J. T. Park, G. Friemel, Y. Li, J. H. Kim, V. Tsurkan, J. Deisenhofer, H.-A. Krug von Nidda, A. Loidl, A. Ivanov, B. Keimer, and D. S. Inosov, Phys. Rev. Lett. **107**, 177005 (2011).

[42]G. Friemel, J. T. Park, T. A. Maier, V. Tsurkan, Y. Li, J. Deisenhofer, H. A. Krugvon Nidda, A. Loidl, A. Ivanov, B. Keimer, and D. S. Inosov, Phys. Rev. B **85**, 140511 (2012).